An Explanation for the Bumps in (p,d), (d,t) and (3He,α) Spectra in Terms of One- and Two-Step Processes

I. 9 An Explanation for the Bumps in (p,d), (d,t) and (^{3}He,α) Spectra in Terms of One- and Two-Step Processes

Ishimatsu T., Tohei T., Hirota J., Morita S., Kawamura T. and Abe K.*
Department of Physics, Faculty of Science, Tohoku University
College of General Education, Tohoku University*

Quite a few studies have been made to correlate broad bumps occurring in (p,d), (d,t) and (^{3}He,α) spectra with deeply-bound neutron-hole states. Ishimatsu et al.[1] carried out an experiment of the (p,d) reactions at 52 MeV on 8 nuclides with neutron numbers ranging from 53 to 82, and made a DWBA analysis of the bumps in the deuteron spectra. They have found that in all the cases the angular distributions for deuterons under the bumps are roughly reproduced both in shape and in magnitude by the calculation on the assumption that the regions of 8 MeV widths under the bumps represent the full spectroscopic strength of the gfp neutron shell consisting of the $1g_{9/2}$, $2p_{1/2}$, $2p_{3/2}$ and $1f_{5/2}$ subshells.

we tried taking account of two-step process to improve the rather poor agreement between experimental data and DW predictions obtained in ref. 1). We also attempted applying the same method of analysis to the bumps from the (d,t) and (^{3}He,α) reactions. The experimental data analyzed here are: (i) The data of the (p,d) reactions on ^{98}Mo, ^{116}Cd and ^{124}Sn at 52 MeV taken from ref. 1); (ii) The data of the (d,t) reaction on ^{116}Sn at 50 MeV from ref. 2); (iii) The data of the (^{3}He,α) reaction on ^{116}Sn at 65 MeV, which we have measured with the CYRIC cyclotron and a conventional SSD telescope system.

We define after ref. 1) a "bump region" as the spectral region of 8.0 MeV width that extends toward higher excitation energies from a distinct valley between the bump in question and the structure resulting from the pick-up of valence neutron. The region between two hatched lines in each spectrum shown in fig. 1 is the bump region defined in this way. We anticipate that the bump region virtually represents the full neutron-hole strength of the gpf shell from the following reasons: (i) Calculated energies[3,4] of a single neutron in a Woods-Saxon potential suggest that for nuclei in a mass region relevant to the present report, the range of strength distribution of the gpf neutron shell is about 8 MeV irrespectively of nuclear mass. (ii) It is naturally expected that the $1g_{7/2}$ and $1g_{9/2}$ neutron-hole strengths overlap around one boundary of the bump region and the $1f_{5/2}$ and $1f_{7/2}$ neutron-hole strengths around the other; still, the bump region will behave as far as its angular distribution is concerned as if it includes nearly full strengths of the $1g_{9/2}$ and $1f_{5/2}$ neutron-hole states for the only ℓ=4 and 3 components, respectively, when its boundaries are chosen at appropriate locations.

Open circles in figs. 2 and 3 represent the experimental differential cross sections for the bump regions. Statistical uncertainties of the data are always smaller than the size of the circles. Locations of the bump regions expressed

in residual excitation are inserted in these figures. In the case of the $^{116}Sn(d,t)^{115}Sn$ reaction, the width of the bump region is taken to be 8.75 MeV, and the triton spectra shown in ref. 2) suggest that the experimental cross sections given in fig. 3 decrease by about 5 % when the width is taken to be 8.0 MeV as in the other cases.

It is expected from the above discussion that the angular distribution of the bump region includes as a main component the contribution of full-strength one-step transitions to the neutron-hole states in the gpf shell. In addition to this, another contribution may be appreciable; i.e., the contribution of two-step transitions involving the neutron pick-up from the gpf shell and the inelastic excitation of the first 2^+ and 3^- states in the target or core nucleus. A schematic diagram of the two-step process is shown in fig. 4. It is plausible from a consideration of energy that the bump region includes also most of the reaction particles that leave residual nuclei in the states resulting from the hole-core coupling in question.

We have calculated the cross sections for the full-strength one-step transitions to the neutron hole states in the gpf shell and those for the full-strength two-step transitions to the states resulting from the coupling of the gpf neutron-hole states to the first 2^+ and 3^- states in the target nucleus. Each of the curves shown in figs. 2 and 3 represents the sum of these calculated cross sections.

The calculations were performed with the code CHUCK[5]. The optical-model parameters used in the calculations for the (p,d) reactions on ^{98}Mo, ^{116}Cd and ^{124}Sn were the same as used in ref. 1), and those for the $^{116}Sn(d,t)^{115}Sn$ reaction the same as used in ref. 2). For the $^{116}Sn(^3He,\alpha)^{115}Sn$ reaction, the optical-model parameters were taken from ref. 6), a study of the $^{144}Sm(^3He,\alpha)^{143}Sm$ reaction at 30 MeV. In each of the residual nuclei, the $1g_{9/2}$ neutron-hole state is tentatively assumed to be at the position of maximum yield in the bump region, which is virtually independent of observation angle and reaction type, and the $2p_{1/2}$, $2p_{3/2}$ and $1f_{5/2}$ neutron-hole states at the middle of the bump region; the assumed positions are listed in table 1. The deformation parameters β_ℓ for the inelastic excitation of the first 2^+ and 3^- states in the target nuclei used in the present calculation are listed in table 2; the data for ^{98}Mo are from a study[7] of inelastic scattering of 15 MeV protons, those for ^{116}Cd from a study[8] of inelastic scattering of 12 MeV protons, and those for ^{116}Sn and ^{124}Sn from a study[9] of inelastic scattering of 24.5 MeV protons.

The contributions of the one- and two-step processes for the $^{116}Sn(d,t)^{115}Sn$ reaction are separately shown in fig. 5, where σ_o represents the sum of the calculated cross sections for the full-strength one-step transitions to the gpf neutron-hole states, and σ_t the sum of the cross sections for the full-strength two-step transitions to the states resulting from the coupling of the gpf neutron holes to the first 2^+ and 3^- states in the target (core) nucleus. Curves a and b stand for the contributions of the two-step processes

involving the 2^+ and 3^- states, respectively, and the solid curve represents the sum of the one- and two-step contributions, σ_o and σ_t, which is identical with the curve shown in the lower part of fig. 3.

Figs. 2 and 3 show that the angular distributions for the bumps in (p,d), (d,t) and (^{3}He,α) spectra are reproduced fairly well by the present calculation both in shape and in magnitude in a systematic way without assuming no background of unknown origin. This seems surprising in view of the simple and rather crude assumptions used in the calculation.

References

1) Ishimatsu T., Niwano M., Kawamura N., Ohmura H. and Awaya T., Nucl. Phys. A336 (1980) 205.
2) van der Werf S. Y., Harakeh M. N., Put L. W., Scholten O. and Siemssen R. H., Nucl. Phys. A289 (1977) 141.
3) Bohr A. and Mottelson B. R., Nuclear structure, Vol. 1 (Benjamin, New York, 1969) p. 239.
4) Hodgson P. E., Nuclear reactions and nuclear structure (Clarendon press, Oxford, 1971) p. 19.
5) Kunz P. D., unpublished.
6) Friedland E., Goldschmidt M., Wiedner C. A., Ford J. L. C., Jr. and Thornton S. T., Nucl. Phys. A256 (1976) 93.
7) Lutz H. F., Heikkinen D. W. and Bartolini W., Phys. Rev. C 4 (1971) 934.
8) Deye J. A., Robinson R. L. and Ford J. L. C., Jr., Nucl. Phys. A180 (1972) 449.
9) Beer O., El Behay A., Lopato P., Terrien Y., Vallois G. and Seth K. K., Nucl. Phys. A147 (1970) 326.

Table 1. Excitation energies in MeV of the neutron hole states in the residual nuclei assumed in the present calculation

	^{97}Mo	^{115}Cd	^{115}Sn	^{123}Sn
$(1g_{9/2})^{-1}$	3.5	4.5	5.5	5.8
$(2p_{1/2})^{-1}$	5.7	7.1	7.5	8.0
$(2p_{3/2})^{-1}$	5.7	7.1	7.5	8.0
$(1f_{5/2})^{-1}$	5.7	7.1	7.5	8.0

Table 2. Deformation parameters β_ℓ for inelastic excitation of the first 2^+ and 3^- levels in the target nuclei used in the present calculation

	^{98}Mo	^{116}Cd	^{116}Sn	^{124}Sn
β_2	0.168[a)]	0.195[b)]	0.143[c)]	0.119[c)]
β_3	0.195[a)]	0.139[b)]	0.188[c)]	0.138[c)]

a) Ref. 7).
b) Ref. 8).
c) Ref. 9).

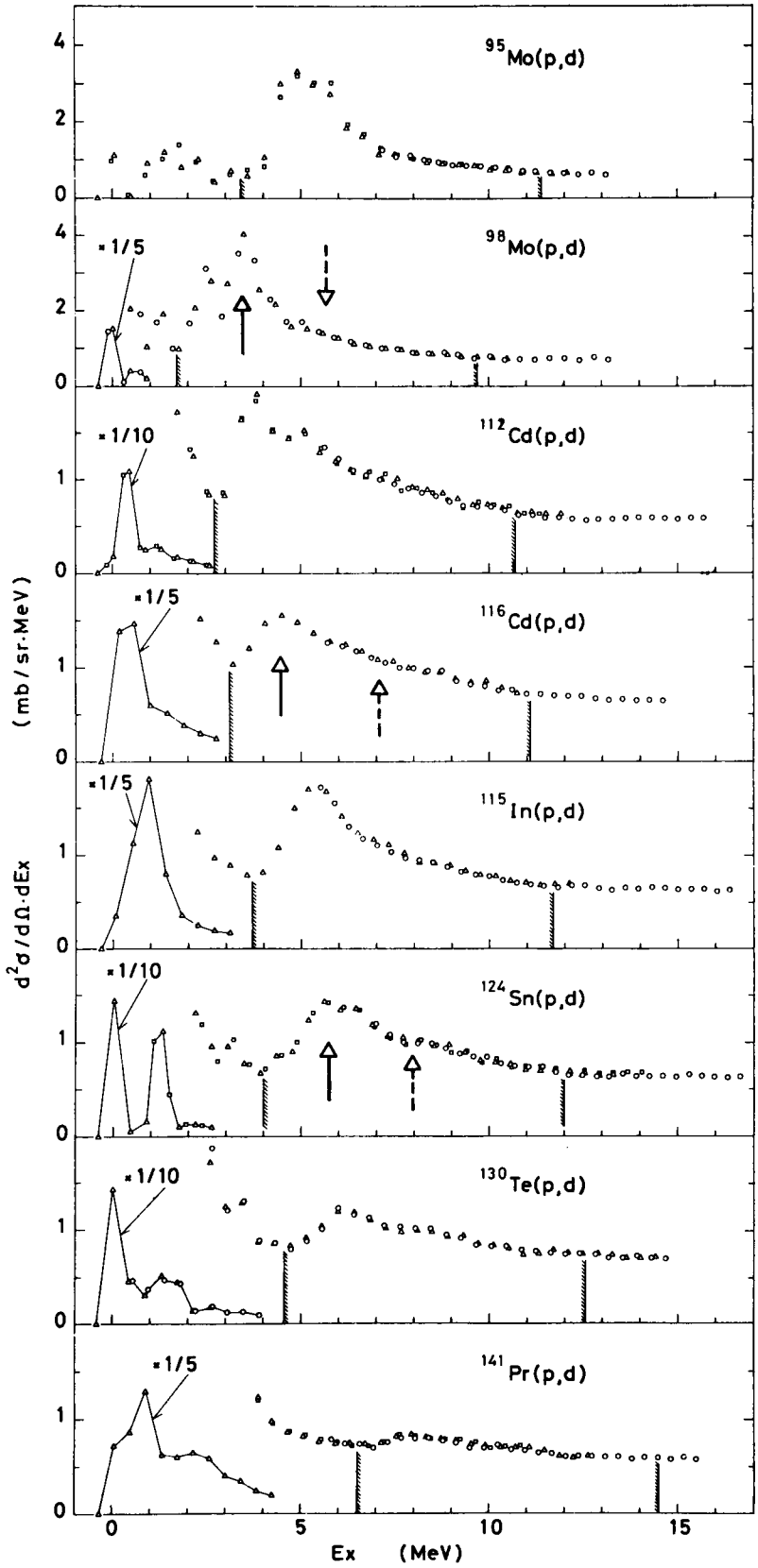

Fig. 1. Deutron spectra from (p,d) reactions at 52 MeV measured at a lab angle of 20° [ref. 1)].

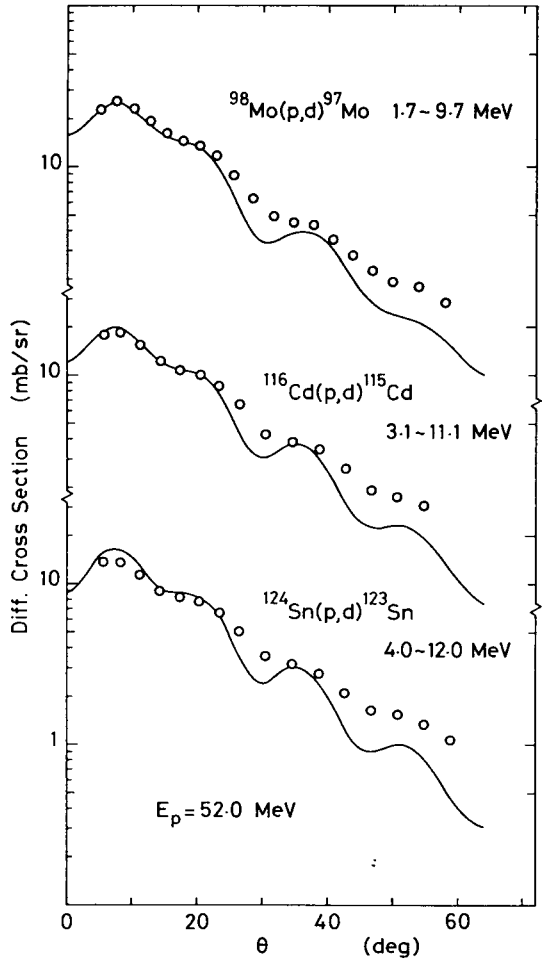

Fig. 2. Comparison of calculated differential cross sections with experimental data for the (p,d) reactions on ^{98}Mo, ^{116}Cd and ^{124}Sn at 52 MeV.[1)]

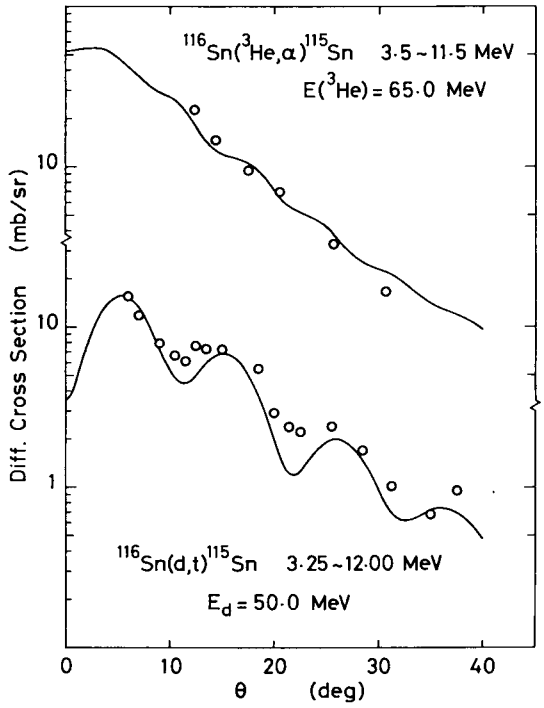

Fig. 3. Comparison of calculated differential cross sections with experimental data for the ^{116}Sn(d,t)^{115}Sn reaction at 50 MeV[2)] and the ^{116}Sn (^{3}He,α)^{115}Sn reaction at 65 MeV.

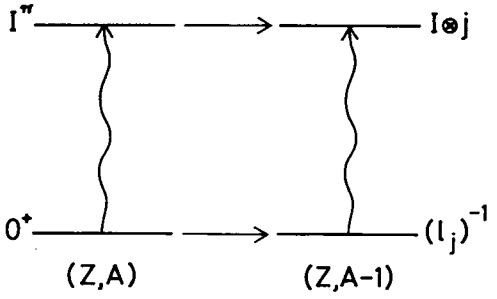

Fig. 4. A schematic diagram of the two-step process taken into account in the present analysis.

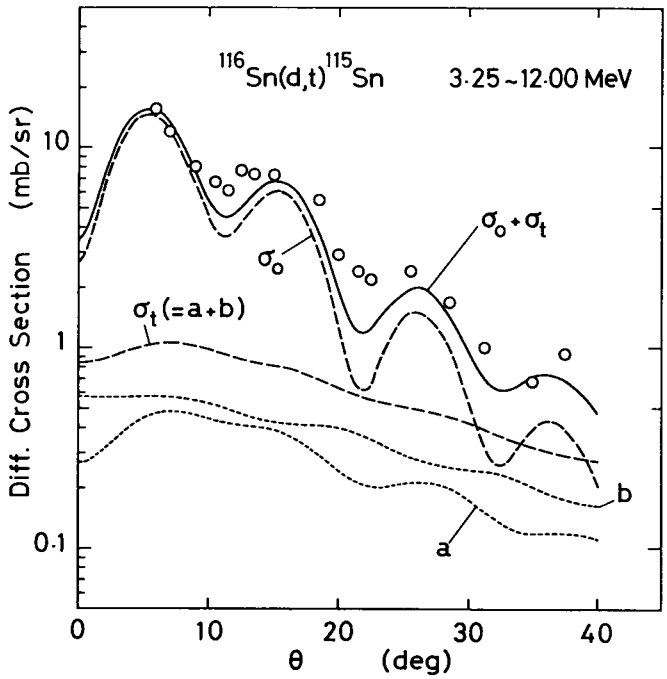

Fig. 5. Comparison of calculated differential cross sections with experimental data for the $^{116}Sn(d,t)^{115}Sn$ reaction at 50 MeV.[2)]